AIAA 94-2596
Lift, Drag and Thrust Measurement in a Hypersonic Impulse Facility

S.L. Tuttle, D.J. Mee and J.M. Simmons
Department of Mechanical Engineering
The University of Queensland
Brisbane, Australia

18th AIAA Aerospace Ground Testing Conference
June 20-23, 1994 / Colorado Springs, CO

LIFT, DRAG AND THRUST MEASUREMENT IN A HYPERSONIC IMPULSE FACILITY

S.L. Tuttle *, D.J. Mee ** and J.M. Simmons ***

The University of Queensland, Australia

Abstract

This paper reports the extension of the stress wave force balance to the measurement of forces on models which are non-axisymmetric or which have non-axisymmetric load distributions. Recent results are presented which demonstrate the performance of the stress wave force balance for drag measurement, for three-component force measurement and preliminary results for thrust measurement on a two-dimensional scramjet nozzle. In all cases, the balances respond within a few hundred microseconds.

1. Introduction

A new technique has been developed at The University of Queensland for measuring the transient forces experienced by models in the hypersonic flows of the T4 free piston driver shock tunnel. In this facility, where test flow durations of 1 millisecond are typical, there is usually insufficient time for the model to reach a state of force equilibrium with its supports. However, by interpretation of the stress waves which travel through the supports, the aerodynamic loading may be determined. This is achieved by studying the dynamic behaviour of the model on its support using finite element analysis and dynamic calibration. In this paper the capabilities of the stress wave force balance for measurement of drag on an axisymmetric body are first demonstrated using recent measurements on a long (425 mm) 5° semi-vertex angle cone at zero incidence. Results are then presented from tests in which a 15° cone was placed at incidence, producing non-axisymmetric forces on the model. Three components of force were measured. Finally, preliminary results are presented for measurements of the thrust produced on an 11° scramjet thrust nozzle of rectangular cross-section.

2. The Force Measurement Technique

The measurement of forces on vehicles flying at hypervelocity conditions has been restricted by the short durations for which current experimental facilities can sustain a representative flow. Progress has recently been made in designing balances for use in flows of duration as short as a few milliseconds[1,2,3].

Conventional force balances require sufficient test time for the forces on the model and its supports to reach equilibrium. Acceleration compensation has enabled the measurement of forces in test times as short as 10 milliseconds. For the 1 millisecond test flows of hypervelocity impulse devices such as T4, the flexibility of the model becomes significant and these methods do not work. The use of discrete pressure tappings for inferring forces is limited to simple model geometries and does not take account of skin friction.

The configuration of the stress wave force balance is shown in Figure 1. The model is mounted on a long support, or sting, and the two are suspended freely from the test section roof by fine wires. The model is aligned with the flow direction.

The impact of the flow on the model causes stress waves to travel through the model and on into its support. Tension and compression stress waves travel at the speed of sound of the material. An important feature of this force measurement technique is that the sting is made long enough to allow sufficient time for the rise of the stress in the sting to be measured before the reflection of the initial waves returns from the far end of the sting. To this end, strain gauges are mounted on the sting a short distance behind the model.

In the case of drag measurement, the impact of the flow on the model causes compression waves to travel through the model. Upon arrival at the interface with the sting, some of these waves will reflect from this boundary and some will be transmitted into the sting. The stresses continue to reflect within the model while the waves

---

* Graduate student, Department of Mechanical Engineering

** Lecturer, Department of Mechanical Engineering

*** Dean of Engineering, MAIAA

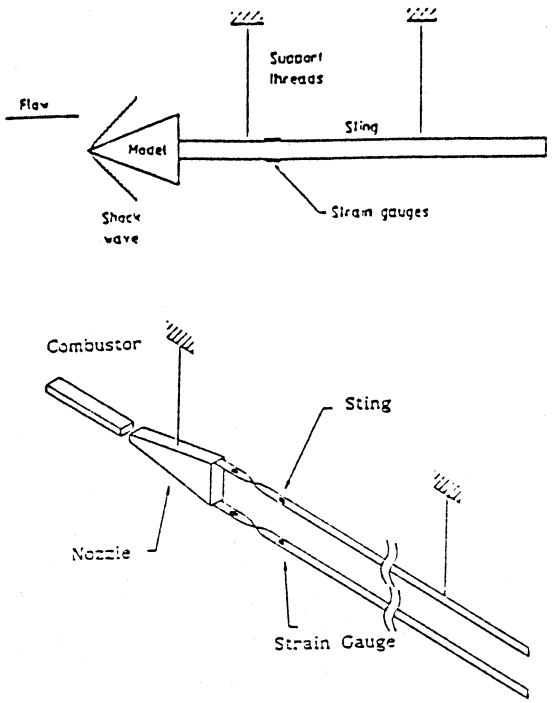

Fig. 1 Stress wave balance configuration for a cone model and a scramjet thrust nozzle.

propagating down the sting will reflect from the free end as tension waves. Materials are chosen so that the stress waves pass through the model as quickly as possible, and are then slowed down in the sting to maximise observation time. Aluminium (stress wave speed = 5000 m/s) is used for the model and brass for the sting (stress wave speed = 3500 m/s). The sting is 2 metres long and so there are approximately 1.1 milliseconds before the reflected stress waves returns.

The joint between the model and sting is important. The impedance of this should be minimised. This entails maximising the contact area between the two and minimising the mass of the model, while still ensuring that the level of strain in the sting is measurable.

The rise of the stress at the strain gauge position due to a step loading on the model may be approximated as exponential[4] with the following time constant, τ

$$\frac{m}{\rho c A}$$

where m is the mass of the model, ρ is the density of the sting material, c is the speed of sound in the sting material and A is the contact area between the model and sting. It is desirable to keep the time constant as small as possible, so the contact area needs to be as large as possible and the model should not be excessively heavy. However, the balance does allow the testing of models of a useful size.

Generally, the level of stress in the sting does not reach the static or steady state level that would be reached if the tunnel loading lasted longer. In order to determine what the actual aerodynamic load was that caused the response measured in the sting, a knowledge of the impulse response of the model is required. This is obtained experimentally by dynamic calibration and is then compared with a finite element prediction. The dynamic calibration involves suspending the model and sting vertically. Weights are hung from the model by a thin wire. Cutting the wire provides a step change in the load on the model.

It is possible to obtain an impulse response which includes the reflections of the stress waves off the model and the ends of the stings. By cutting a support wire and allowing the model and sting to fall freely under their own weight, a free-end condition is achieved for the stings. This allows the deconvolution of the aerodynamic loading over longer times (even though the useable test flow in the tunnel usually finishes at approximately the same time that the first stress wave reflection returns).

The MSC/NASTRAN package is used to compute the response of the model to a step pressure load. The impulse response is then the derivative of the step response. It has been shown that both the 5° semi-vertex angle cone and the thrust nozzle are reasonably insensitive to loading distribution, by comparing the extremes of a point load applied at one end of the model, and a uniformly distributed pressure loading applied to the appropriate model surfaces.

The model on its sting is a linear dynamic system which may be described by the following convolution integral:

$$y(t) = \int_0^t g(t-\tau)\, u(\tau) d\tau$$

where y(t) is the strain measured in the sting, u(t) is the input drag or thrust, and g(t) is the unit impulse response of the system. Once g(t) is known for the system, the unknown loading on the model may be found by deconvolution. An iterative time domain deconvolution algorithm of Prost and Goutte[5] is used.

The stress wave force balance was initially demonstrated by Sanderson and Simmons[6] using a 200 mm long 15° semi-vertex angle cone. The 425 mm long 5° cone represents a more demanding test of the technique. The greater length means that stress wave reflections within the model occur over a longer time and the geometry of the cone means that the total drag forces being measured are smaller. Both skin friction and base pressure

become important factors. Early results from this model have been shown by Sanderson et al.[4] More recent results demonstrating the performance of the balance for an axisymmetric loading on an axisymmetric model are shown next.

3. Results

(a) Drag on the 5° Semi-Angle Cone

Figure 2 shows the deconvolved, measured drag on the 5° cone compared with a theoretical prediction using Taylor-Maccoll[7] cone flow theory, a skin friction approximation and a base pressure approximation. The skin friction is assessed using a reference temperature method and Sutherland's viscosity law. An entirely laminar boundary layer is assumed. The base flow is complicated by the presence of the sting and a buffer placed within 2 mm of the base of the cone. Base pressure is approximated by assuming the flow between the base and the plastic buffer located just behind the model is choked. The strain time histories measured in the sting were deconvolved using an experimentally obtained impulse response. The deconvolution process amplifies the experimental noise, so the results have been filtered with an 8-pole Butterworth low-pass filter with a cut-off frequency of 2 kHz. The test time in T4 is designated as the period in which the ratio of Pitot to stagnation pressure is constant. The tunnel was operated with a Mach 5 contoured nozzle and near-tailored conditions are attained for approximately one millisecond.

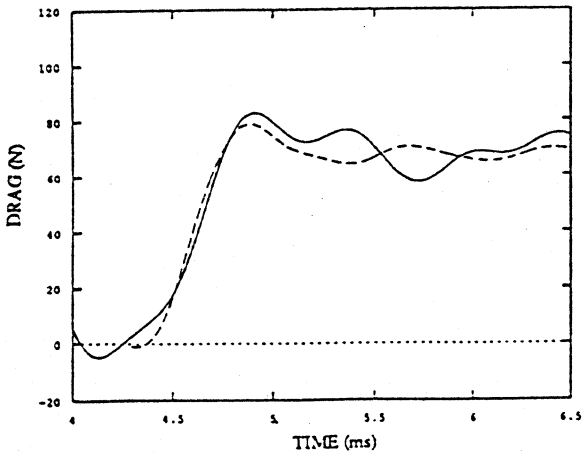

Nozzle supply conditions : enthalpy = 3.4 MJ/kg, pressure = 35.2 MPa; freestream conditions : pressure = 8.94 kPa, temperature = 344 K, velocity = 2390 m/s, density = .04956 kg/m^3, γ = 1.39.

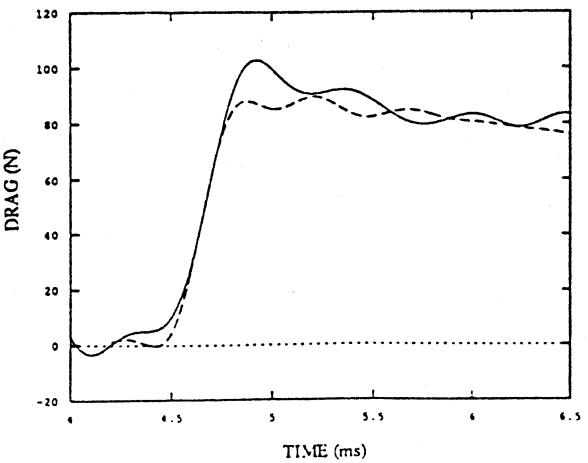

Nozzle supply conditions : enthalpy = 6.8 MJ/kg, pressure = 43.6 MPa; freestream conditions : pressure = 11.5 kPa, temperature = 781 K, velocity = 3446 m/s, density = .0905 kg/m^3 , γ = 1.36.

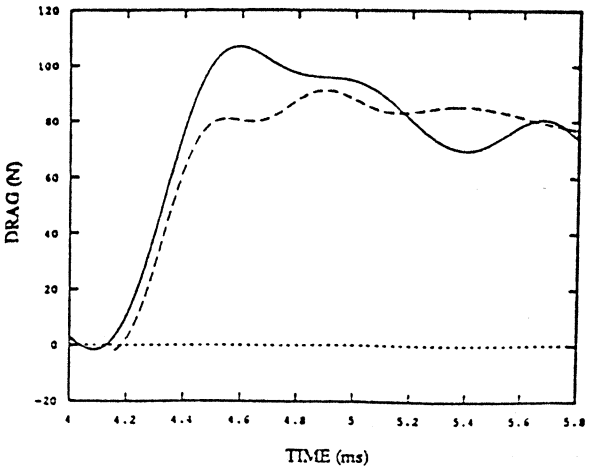

Nozzle supply conditions : enthalpy = 11.3 MJ/kg, pressure = 41.5 MPa; freestream conditions : pressure = 12.2 kPa, temperature = 1410 K, velocity = 4389 m/s, density = .0291 kg/m^3, γ = 1.32.

Fig2. Comparison of experimental and theoretical drag on a 5° cone at zero incidence.
_____ deconvolved measured drag
- - - - - theoretical drag

The test gas is nitrogen. This eliminates dissociation effects. Results were obtained for three different nozzle supply enthalpies. The nozzle supply enthalpy is varied by varying the pressure of the test gas in the shock tube. The nozzle supply pressure is varied by changing the thickness of the steel primary diaphragm between the driver and shock tubes. Results were obtained for nozzle supply enthalpies from 3 to 13 MJ/kg for two primary diaphragm thicknesses (4 and 5 mm). The results are summarised in Figure 3 in terms of drag

coefficient. The reference area for the coefficient is the base area of the cone.

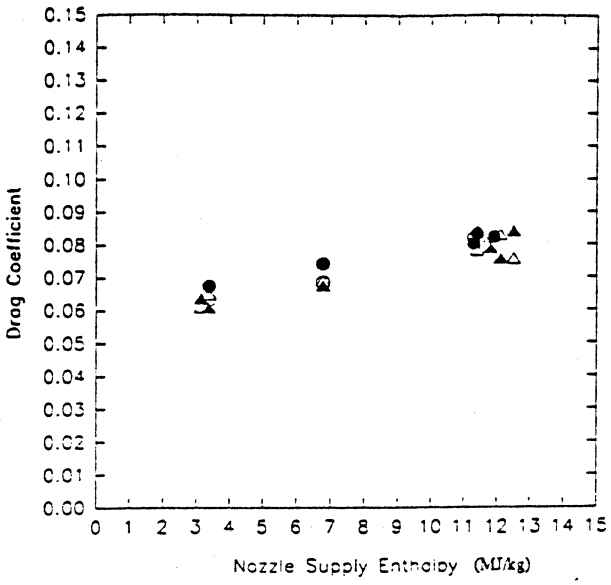

Fig. 3 Variation of drag coefficient with nozzle supply enthalpy for a 5° cone at zero incidence.

A single value of drag is obtained for each shot by averaging the signals over a 300 μs period from the start of the test time. The theoretical levels (open symbols) are compared with the experimental results (closed symbols). The triangles represent the lower pressure 4mm diaphragm condition and the circles are the high pressure 5 mm conditions. Very good agreement is observed (within 10%) and a trend of increasing drag coefficient with increasing supply enthalpy is apparent. This trend can be associated with the performance of the nozzle. The Mach number of the flow exiting the nozzle changes with nozzle supply enthalpy due to differences in the behaviour of the test gas at high temperature (the gas may not expand in chemical equilibrium) and because of possible differences in the growth of the nozzle boundary layers. The exit Mach number decreases with nozzle supply enthalpy over the range of the present experiments. The components of the drag coefficient associated with surface pressure and with skin friction both increase with nozzle supply enthalpy.

(b) Three-Component Force Measurement

The viability of the stress wave balance was demonstrated by the uniaxial drag measurement on the initial 15° cone and the 5° cone described above. The technique has been extended to the simultaneous measurement of several components of force, namely lift, drag and pitching moment.

The major modification here is in the method of attachment of the model to the sting. The aim is to minimise the coupling amongst signals which are used to determine the axial and normal forces and the pitching moment.

The three-component deconvolution force balance consists of a single, 2 m long sting attached to the test model by four short bars (Figure 4). Each of the short bars is instrumented for measurement of axial strain at its mid-point. A strain gauge bridge is also attached to the sting 200 mm from the model/sting junction. Combinations of the strain signals from the four bars are used to produce two output signals - one responding primarily to an axial force input signal and the other responding primarily to a pitching moment input signal. The strain measurement in the sting responds primarily to an axial force input. Inevitably there is some coupling amongst these output signals.

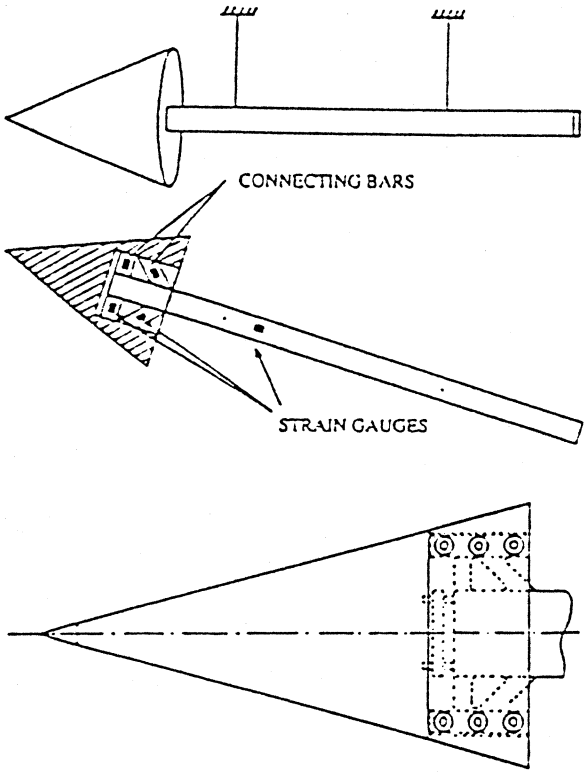

Fig. 4 Three component balance with details of the connection to the sting.

The time histories of the three outputs related to axial and normal forces and moment, $y_A(t)$, $y_N(t)$ and $y_M(t)$, can be related to the time-histories of the axial force, normal force and pitching moment on the model, $u_A(t)$, $u_N(t)$ and $u_M(t)$ via nine impulse response functions. This coupled convolution problem can be written in matrix notation as in Mee et al.[8]

$$\begin{pmatrix} y_A \\ y_N \\ y_M \end{pmatrix} = \begin{pmatrix} G_{AA} & G_{AN} & G_{AM} \\ G_{NA} & G_{NN} & G_{NM} \\ G_{MA} & G_{MN} & G_{MM} \end{pmatrix} \begin{pmatrix} u_A \\ u_N \\ u_M \end{pmatrix}$$

where the y vectors are formed from the discretised output signals and the u vectors are formed form the applied load time histories. The square G matrices are formed from the impulse response functions, G_{ij} being the impulse response for the y_i output to a u_j input. If there is no coupling amongst the outputs then the off-diagonal submatrices in the impulse response matrix will be null.

The nine impulse response matrices are obtained by a series of bench test in which a weight is attached to various points of the model by a fine wire and then quickly released. The output strain signals are processed to produce the impulse responses. The linearity of the system enables the responses to flow-type loading distributions to be determined by superposition of the results of several tests for single loads applied at various locations on the model.

In experiments in the shock tunnel, each of the y_i outputs is measured and time domain, coupled deconvolution techniques are used to determine the time histories of the lift and drag forces and pitching moment on the model. The experimentally determined impulse response functions are used for this deconvolution.

The prototype three-component balance was installed in a 220 mm long, 15° semi-angle, aluminium cone as shown in Figure 4. The cone mass is 1.94 kg. This configuration was also found to be quite insensitive to loading distribution.

Experiments were performed to measure the three components of force on the 15° cone for incidences of 0.0°, 2.5° and 5.0°. Sample results are presented for a nozzle supply enthalpy of 6 MJ/kg in Figure 5. Shown are the deconvolved axial and normal forces and pitching moment as well as the measured Pitot pressure in the test section. The zero for moment has been taken at a point one third of the cone height from the base of the cone, on the axis. (The theoretical line of action of force for a conical, inviscid flow is about 5% of the cone height closer to the base.) A negative moment with a positive normal force indicates the line of action of the net force is closer to the base than the nominal location. All results have been digitally low-pass filtered with a 4-pole Butterworth filter at a cut-frequency of 5 kHz. The vertical line on each plot indicates the time at which nozzle starting is complete and the commencement of steady test flow (based on a constant ratio of Pitot to supply pressures).

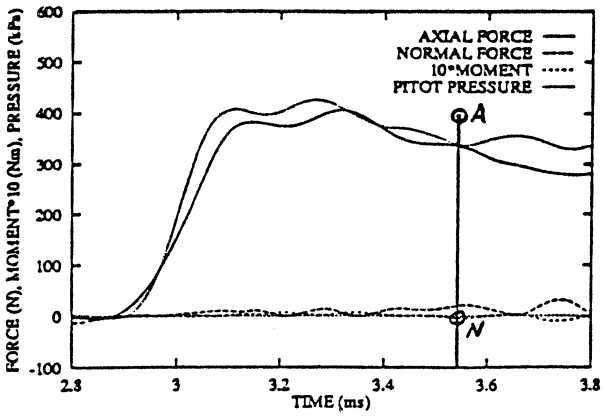

(a) 0.0° incidence

Fig. 5 Deconvolved force and moment time histories. Nozzle supply conditions : enthalpy = 6.5 MJ/kg, pressure = 25 MPa; freestream conditions : temperature = 800 K, velocity = 3400 m/s, density = .033 kg/m^3, γ = 1.36.

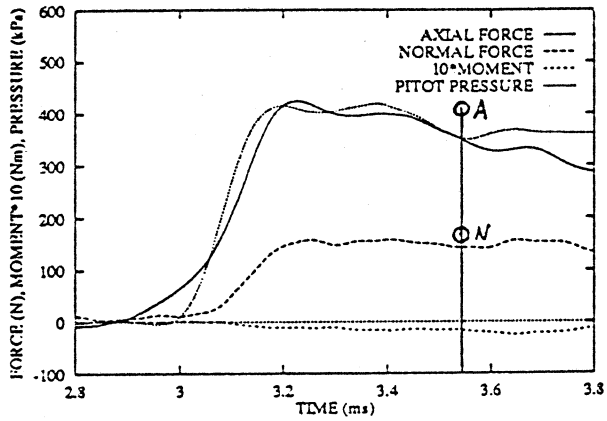

(b) 2.5° incidence

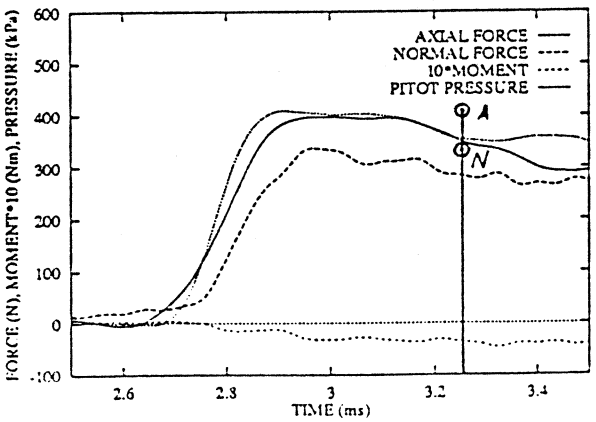

(c) 5.0° incidence

The response of the balance is seen to be good with the axial and normal forces showing time histories similar to the Pitot pressure. The current arrangement is such that there are about 800 μs before the waves reflected from the end of the sting return to the locations of strain measurement and interfere with the measurements. This can be seen in the deconvolved axial force signals where the level drops shortly after the measurement time. A longer sting would overcome this limitation on measurement time.

The experimental results are compared with computations of Jones[9]. He presents results of calculations of the axial and normal forces on cones at small angles of attack for various supersonic and hypersonic Mach numbers. The computations are for an inviscid flow of a perfect gas with a ratio of specific heats γ, of 1.4. (γ = 1.36 in the present experiments.) Interpolating on his results, predicted axial and normal forces are compared with the present measurements and are indicated on the plots of Figure 5 with "*A*" for axial force and "*N*" for normal force. There are experimental uncertainties in the conditions of the flow in the test section which may lead, for example, to an uncertainty in axial force of ±12%[10]. While the measured levels of force are about 15% lower than the computations of Jones, the ratios of axial to normal force agree well (to within 5% at this condition). The experimental line of action of force is within 1% of the inviscid, conical flow value for this condition. The overall accuracy of the balance has not yet been quantified.

(c) Scramjet Thrust Measurement

The two-dimensional thrust nozzle presents a challenging problem. The loading is not axisymmetric as in the case of a cone at zero incidence and the internal flow presents some design difficulties. A two-sting system has been chosen to accommodate the internal flow and achieve some symmetry. This can be seen in Figure 1. The nozzle is 300 mm long and together the nozzle and stings weigh 6.55 kg. The angle of the ramp walls is 11° and the area ratio is 4.76.

The situation is complicated by the fact that with the small ramp angle and the internal pressure on the nozzle walls, loading is predominantly transverse. Yet it is the axial thrust which is to be measured through detection of the tensile waves propagating in the stings. Although bending stress waves travel at most at only 60% of the speed of the axial stress waves, the system needs to be stiffened against bending. The second sting is only used to preserve symmetry. Thus, a redundant measurement is also obtained. The expected axial thrust from this nozzle is not large so thin stings are required. In addition to this, the contact area between nozzle and sting needs to be maximised. The result was that it was decided to twist the stings through 90°, without distorting their cross-sectional shape, just aft of the nozzle. This is discussed further in Simmons et al.[11]

Finite element analysis showed that this would not significantly alter the propagation of the axial stress wave in the sting, while the rigidity of the system is greatly increased.

Figure 6 shows the numerically predicted response of the nozzle to a step point load and the experimentally measured step response to a point load. The results indicate that the speed of response of the balance is adequate. The agreement between the computed and experimental responses is quite good. However, the unloading waves arrive approximately 50 μs earlier in the computation. This is possibly due to the material properties for the sting (such as Young's Modulus which determines stress wave speed) not being exactly correct for the particular brass being used for the stings.

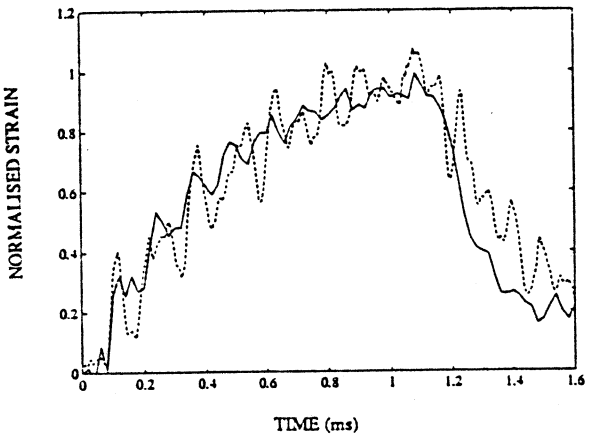

Fig. 6 Comparison of experimental and computational responses of the 11° thrust nozzle to a step point load at the nozzle front.
. . . . . experimental
——— computational

The 300 mm long nozzle is freely suspended behind a fixed scramjet combustor. A Mach 4 contoured nozzle supplies the test gas to the combustion duct. Fuel is injected at the entrance to the duct from a two-dimensional central, planar strut. The combustor duct is 600 mm long. A 3 mm lip at the exit of the combustor will ensure there is no flow leakage, while simultaneously allowing free movement of the nozzle and stings. Around the perimeter of the lip there is approximately 0.5 mm of clearance with the nozzle. This is shown in Figure 7.

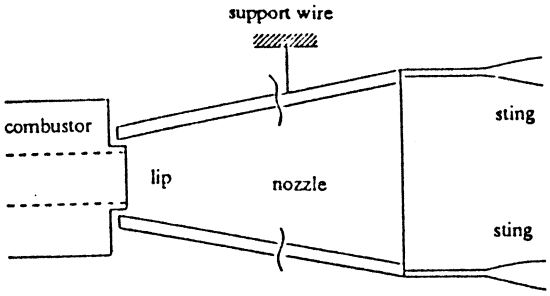

Fig. 7 Details of the join between the thrust nozzle and combustor.

The alignment of the nozzle behind the combustor has been one of the challenges of this experiment. Sufficient free movement is required to measure signals of a useful duration (production of positive thrust will accelerate the nozzle towards the combustor) while flow leakage onto the front face of the nozzle is undesirable.

The stings are mounted into the top surface of the nozzle ramp walls in order to keep them out of the nozzle exit plane (see Figure 7). The nozzle is shielded from the external flow and the two stings are shielded from the nozzle exit flow.

There are static pressure tappings in the ramp walls of the nozzle and a Pitot rake provides a survey of the flow at the exit of the nozzle. Combustor static pressures are also measured, and shots are repeated with the nozzle removed in order to measure the Pitot pressure across the combustor exit.

The thrust measured via the strain gauges will be the net axial load on the nozzle. This should be less than the thrust calculated from static pressure measurements by an amount equal to the skin friction. The skin friction is inferred by using a friction coefficient of .003 taken from the computations of nozzle skin friction by Schetz[12]. The Pitot pressure at ten locations down the nozzle is approximated from the measured exit values assuming isentropic flow through the nozzle. Hence the calculated skin friction will only be approximate.

Figure 8 shows the static pressure distribution down the nozzle ramp wall, while Figure 9 shows the Pitot pressure profile across the nozzle exit plane. These distributions are shown for three cases: hydrogen fuel injected into air (combustion), air with no fuel and hydrogen fuel injected into nitrogen (mixing). The shock tunnel nozzle supply enthalpy is 9 MJ/kg.

At this stage, the deconvolved signals are typically marred by large, oscillations. An example of this is shown in Figure 10, where the inferred net load on the nozzle is compared with the deconvolved strain measurement of the thrust.

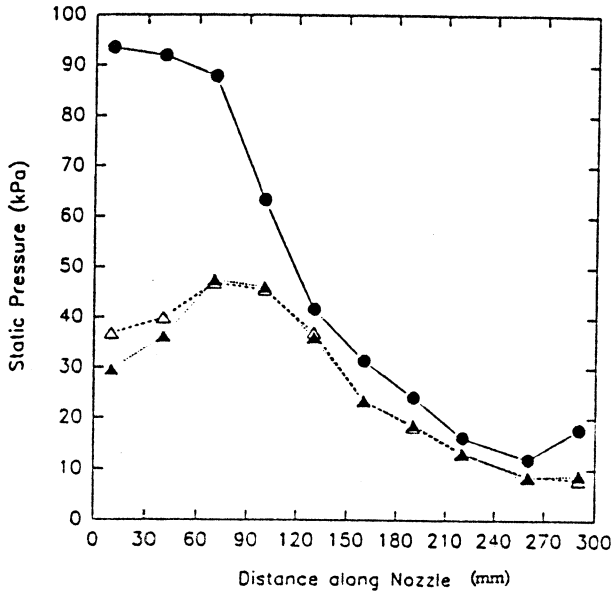

Fig. 8 Static pressures in the thrust nozzle.

● - combustion
△ - mixing
▲ - air only

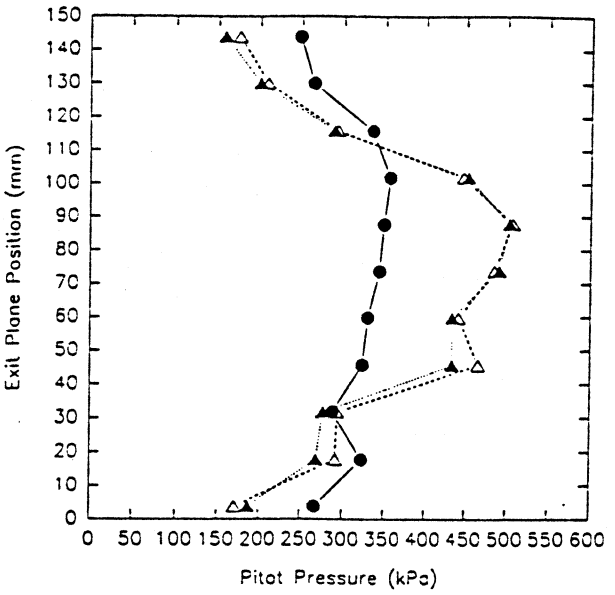

Fig. 9 Pitot pressures across the nozzle exit.

● - combustion
△ - mixing
▲ - air only

When these signals are filtered heavily, it can be seen that the mean level compares favourably with the net load inferred from the pressure

measurements and skin friction approximation. These oscillations are not introduced through the deconvolution and their source is currently being investigated. The general agreement in level is encouraging, but further testing and analysis is required.

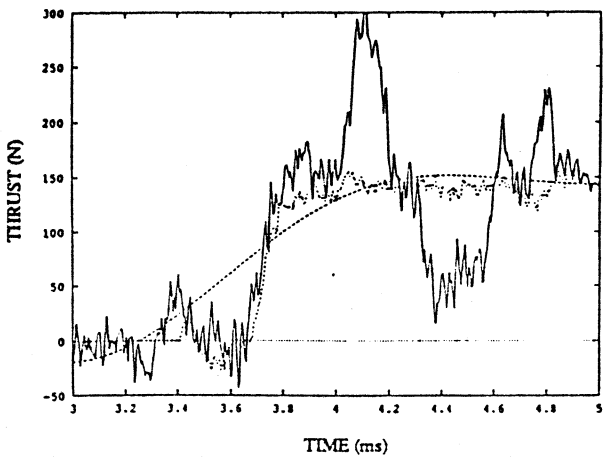

Fig. 10 Deconvolved thrust signal compared with net thrust inferred from pressure measurements and a skin friction approximation.
____ unfiltered deconvolved thrust signal
- - - - filtered deconvolved thrust signal
. . . . . inferred net thrust

4. Conclusions

This paper has presented recent measurements made with single and multi-component stress wave force balances. The single component balance produces results in good agreement with predictions. The extension of the balance to measurement of non-axisymmetric loads has also been achieved with measurements of three components of force on a conical model. A balance is also being developed for measurement of the thrust produced by a scramjet nozzle of rectangular cross section. Preliminary results for this configuration show promise, but further development is required.

References

1. Carbonaro, M, "Aerodynamic Force Measurements in the VKI Longshot Hypersonic Facility", *New Trends in Instrumentation for Hypersonic Research*, (ed. A. Boutier), Kluwer, Dordrecht, pp 317-325, 1993.

2. Jessen, C, Gronig, H, "A Six Component Balance for Short Duration Hypersonic Facilities", *New Trends in Instrumentation for Hypersonic Research*, (ed. A. Boutier), Kluwer, Dordrecht, pp 295-305, 1993.

3. Naumann, K W, Ende, H, Mathieu, G, "Millisecond Aerodynamic Force Measurement Technique for High Enthalpy Test Facilities", *New Trends in Instrumentation for Hypersonic Research*, (ed. A. Boutier), Kluwer, Dordrecht, pp 307-316, 1993.

4. Sanderson, S.R., Simmons, J.M., Tuttle, S.L., "A Drag Measurement Technique for Free Piston Shock Tunnels", AIAA-91-0549, 29th Aerospaces Sciences Meeting, Reno, Nevada, Jan. 7-10, 1991.

5. Prost, R., Goutte, R., "Discrete Constrained Iterative Deconvolution Algorithms with Optimised Rate of Convergence", Signal Processing, 7, 209-230, 1984.

6. Sanderson, S.R., Simmons, J.M., "Drag Balance for Hypervelocity Impulse Facilities", AIAA Journal, Vol. 29, No. 12, pp. 2185-2191, December 1991.

7. Taylor, G.I. and Maccoll, J.W., "The Air Pressure on a Cone Moving at High Speed", Proc. Royal Soc. (London), Ser. A, 139, pp 278-297, 1932.

8. Mee, D.J., Daniel, W.J., Tuttle, S.L., Simmons, J.M., "Balances for the Measurement of Multiple Components of Force in flows of a Millisecond Duration", Proc. 19th International Symposium on Shock Waves, 26-30 July, Marseilles, France, 1993.

9. Jones, D.J.," Tables of Inviscid Supersonic Flow about Circular Cones at Incidence, γ = 1.4", AGARDograph 137, 1969.

10. Mee, D.J., "Uncertainty Analysis of Conditions in the Test Section of the T4 Shock Tunnel", Research Report 4/93, Dept. of Mech. Eng., The University of Queensland, 1993.

11. Simmons, J.M., Daniel, W.J., Mee, D.J., and Tuttle, S.L., "Force Measurement in Hypervelocity Impulse Facilities", *New Trends in Instrumentation for Hypersonic Research*, (ed. A. Boutier), Kluwer, Dordrecht, pp 285-294.

12. Schetz, J.A., Billig, F.S., Favin, S., "Numerical Solutions of Scramjet Nozzle Flows", J. Propulsion, Vol. 3, No. 5, 1986.